JOURNAL OF AIRCRAFT
Vol. 36, No. 2, March–April 1999

Pneumatic Lift and Control Surface Technology for High Speed Civil Transports

Robert J. Englar,* Curt S. Niebur,† and Scott D. Gregory†
Georgia Tech Research Institute, Atlanta, Georgia 30332-0844

Experimental evaluations have been conducted of blown high-lift devices and control surfaces applied to improve the low-speed terminal-area performance of generic High Speed Civil Transport (HSCT) aircraft. Plain blown flaps and advanced pneumatic high-lift devices have been integrated into highly swept vortex-dominated wings. These produced large lift increases, as well as significant drag reductions greater than full jet thrust recovery. Because conventional horizontal tails were inadequate to trim these configurations, blown canards were employed. In addition to providing positive lift increments for pitch trim, the canards were found to favorably influence the higher angle-of-attack vortex-lift characteristics of the wings. The downwash from these canards resulted in a delay of wing vortex burst. Details of these investigations and test results that confirm the effectiveness of combined pneumatic high-lift devices and control surfaces on these HSCT aircraft configurations are presented.

Nomenclature

AR	=	wing or canard aspect ratio
C_D	=	drag coefficient
C_L	=	lift coefficient
C_{M50}	=	midchord pitching moment coefficient
C_μ	=	wing momentum (blowing) coefficient, based on S
$C_{\mu c}$	=	canard momentum coefficient, based on S
c	=	local chord length
$\bar{c}$	=	mean aerodynamic chord
c_T	=	tail mean geometric chord
h	=	blowing slot height
i_c	=	canard incidence angle
i_T	=	horizontal tail incidence angle
$\dot{m}$	=	slot blowing mass flow
q	=	freestream dynamic pressure
R, R_1, R_2	=	trailing-edge radii on circulation control configurations
S	=	semispan wing area
t	=	wing thickness
V_H	=	horizontal tail volume coefficient
V_j	=	isentropic blowing jet velocity
α	=	angle of attack
δ_{Flap}, δ_F	=	flap deflection angle
δ_{jet}	=	blowing jet turning angle
Λ	=	leading- or trailing-edge sweep angle

Introduction

VARIOUS forms of blown aerodynamic devices have been evaluated in recent years to augment the low-speed, high-lift characteristics of modern-day aircraft. These aircraft, particularly military configurations, usually have relatively high wing loadings and associated high takeoff and landing speeds with long ground rolls. Use of pneumatic devices[1–5] such as blown flaps, jet flaps, leading-edge blowing, or forebody blowing can augment the wing lift, and reduce terminal-area speeds and distances (ground roll as well as climb-out and approach flight paths). More recently, a concept known as circulation control (CC), which employs tangential blowing over highly rounded small trailing edges, has been shown to greatly augment lift and, thus, improve the takeoff and landing capabilities.[6–12] For the two-dimensional airfoils of subsonic aircraft using this technology,[6,7,9] lift augmentation of 80 times the input blowing momentum has been recorded, as has significant drag reduction caused by jet thrust recovery, prevention of flow separation, and operation at lower angle of attack.

Recent interest in high-speed commercial aircraft, such as the High Speed Civil Transport (HSCT), suggests that this pneumatic technology should greatly benefit these vehicles as well.[10] In addition to high wing loadings, these aircraft also frequently employ vortex lift at high angles of attack during takeoffs and landings. This has required such features as mechanical nose droop for visibility and highly upswept aft fuselage contours for ground clearance. While reduced wing sweep and increased wing planform area can improve low-speed flight, these may hinder high-speed cruise performance. A recent research program conducted at Georgia Tech Research Institute (GTRI), under the sponsorship of NASA Langley Research Center, evaluated the potential of blown aerodynamic devices for both lifting surface and control surface applications to high-speed commercial aircraft. The major goals of this program were as follows.

1) Develop advanced pneumatic high-lift configurations for highly swept wings.

2) Evaluate conventional horizontal tails for trim and stability during vortex-dominated operation, both with and without wing blowing.

3) Evaluate blown canards for pitch trim, vortex control, and lift augmentation.

The following sections will discuss the details of these blown lift and control devices, the experimental evaluations employed, the results of these parametric proof-of-concept investigations, and the potential applications.

Experimental Apparatus, Models, and Test Procedures

In this proof-of-concept evaluation, an existing half-span model at GTRI was deemed representative of a NASA generic HSCT configuration. The comparable configurations are

Presented as Paper 97-0036 at the AIAA 35th Aerospace Sciences Meeting and Exhibit, Reno, NV, Jan. 6–9, 1997; received April 16, 1997; revision received July 25, 1998; accepted for publication Aug. 16, 1998.

*Principal Research Engineer, Aerospace and Transportation Laboratory, Acoustics and Aerodynamics Branch, CCRF, Code 0844. Associate Fellow AIAA.

†Cooperative Education Student, Aerospace and Transportation Laboratory, Acoustics and Aerodynamics Branch, CCRF, Code 0844. Member AIAA.

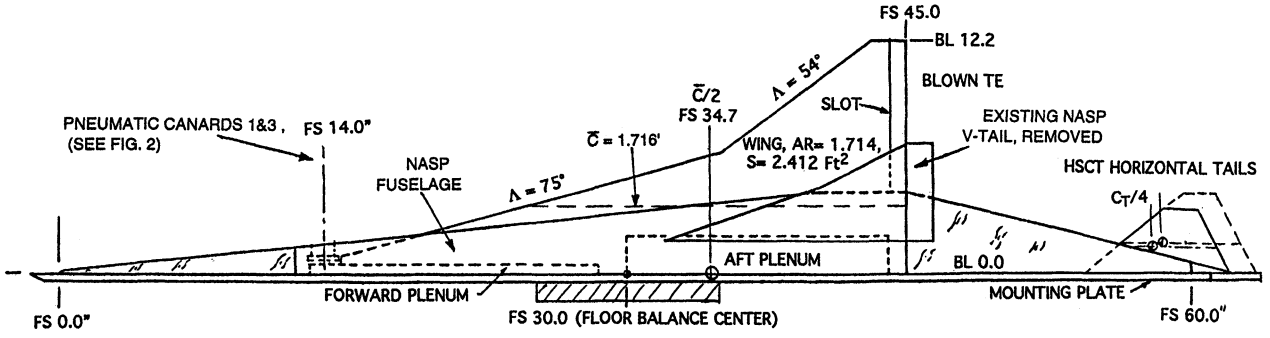

Fig. 1 Planform of the GTRI semispan HSCT/NASP configuration.

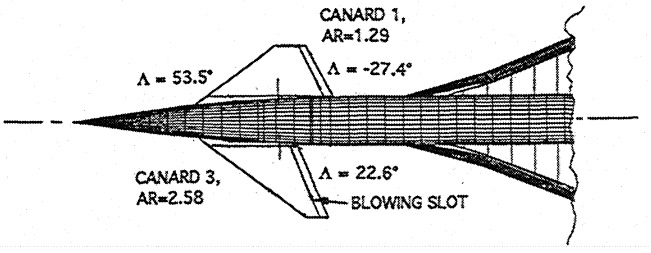

Fig. 2 NASA generic HSCT configuration with Canards 1 and 3.

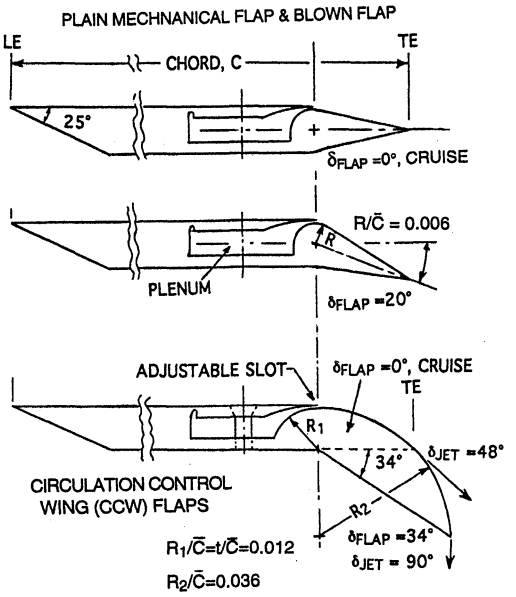

Fig. 3 Blown trailing-edge flap configurations.

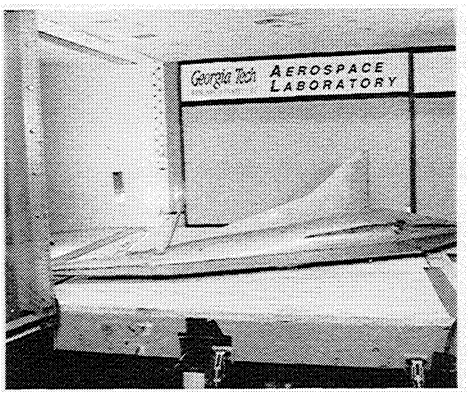

Fig. 4 Semispan generic HSCT model installed at high α in the GTRI Model Test Facility, including Canard 3.

shown in Figs. 1 and 2. The half-span model tested here (Fig. 1) was a generic National Aerospace Plane (NASP) model, which had a wing planform and leading-edge sweeps (75 and 54 deg) similar to current HSCT configurations. The sharply beveled wing leading edge (LE) was intended to generate strong LE vortex flows in the high-lift or high-α modes. The remainder of the main wing airfoil was a flat plate back to the trailing-edge slot (Fig. 3), with a thickness to chord ratio of $t/\bar{c}$ = 0.012 ($\bar{c}$ = 1.716 ft). The wing had a trailing-edge blowing plenum with a tangential slot exiting over the upper surface of a plain flap deflected 20 deg from the chord line. A highly curved CC trailing edge was fabricated to evaluate the effects of larger jet turning on lift augmentation. The undeflected CC *cruise configuration* (0-deg flap) had a curved upper surface yielding 48 deg of jet turning when blown. A 34-deg deflection of the flat lower surface exposed an additional CC arc, producing a total of 90 deg of jet turning. The unblown 20-deg plain flap is representative of conventional HSCT high-lift systems and, thus, serves as a baseline for comparison. The major objective here was to determine blown lift augmentation when operating in the rotational flowfields of the strong vortex from the wing's swept LE.

It was realized that HSCT configurations of this type might well benefit by using a canard to trim with positive lift increment instead of tail download. Thus, two blown canards employing CC-type trailing-edge curvature and tangential blowing were manufactured and employed. Both had curved flap deflections very similar to the CC wing flaps of Fig. 3. These canards, shown in planform in Fig. 2, had similar areas and LE sweep (53.5 deg), but different aspect ratios and trailing-edge sweep. (An intermediate Canard 2 was not evaluated here.) They were tested at various vertical positions above the wing, as well as over a range of incidence, flap angle, and canard blowing coefficients, $C_{\mu c}$. They were located longitudinally 1.005 mean-aerodynamic-chord (MAC) lengths ahead of the wing 0.50 MAC location. The blown plain flap and the CC flaps on the wing were tested at two flap deflections and over a range of wing blowing coefficient values, C_μ.

A series of investigations was conducted to evaluate pitch trim and stability characteristics of conventional horizontal tails. The existing NASP tail was removed (its short moment arm made it very ineffective) and two conventional horizontal tails were fabricated (see Fig. 1). The first, a single-surface configuration without elevators, had a tail area 11.14% of the wing area, and a tail volume coefficient of 0.1312. Also tested was a similar tail geometry with an area increase of 50%, to 16.71% of the wing area, and a tail volume coefficient of 0.2059.

Experimental investigations were conducted in GTRI's Model Test Facility 30 × 43 in. subsonic research wind tunnel, which has been modified for evaluations of semispan pneumatic models with two separate blowing air supplies. The half-span model was installed on a six-component floor-balance whose calibration showed errors less than 1% full-range, and separated from the tunnel wall boundary layer by a splitter plate, as shown in Fig. 4. The floor balance was mounted below a turntable that allowed variation in angle of attack (α) up to 35 deg. The wing and canard were supplied by indepen-

dently controlled air-supply lines passing through separate flow meters and through trapezes to minimize air-pressure tares on the balance. Measured forces and moments at 0.50 MAC were corrected for small-pressure tares and for the interference effects of the splitter plate. In these data, the blowing coefficients for either the wing or the canard are defined as

$$C_\mu = \dot{m}V_j/(qS)$$

Here, V_j is calculated isentropically from measured plenum pressure and temperature. (For this semispan model, that reference area and the aerodynamic forces and moments for only one wing yield full-span three-dimensional coefficients.) $C_{\mu c}$ employs canard mass flow and jet velocity, nondimensionalized by the half-wing reference area and q.

Static flow visualization (wind off) showed that the wing trailing-edge blowing jet sheet adhered to the 20-deg plain flap and deflected 30–35 deg along the inclined upper surface. In comparison, the highly curved CC trailing edge of the blown canard or wing yielded jet turning of nearly 90 deg. Whereas this turning would prove effective in augmenting the canard's lift and providing pitch capability plus a positive lift increment to trim, the real payoff of the blown canard was expected to come from its ability to greatly reduce the upwash flowfield onto the swept-wing LE.

It should be noted there that the strong viscous mixing between the jet, boundary layer, and freestream of CC-type pneumatic devices consumes most of the jet momentum by the time the jet sheet leaves the curved surface. Thus, it is difficult to measure the wind-on thrust of the CC jet and then separate it into lift and drag components caused by thrust, as one can for pure jet flaps. Also, note that for the range of momentum coefficients shown here, jet velocities ranged from low subsonic through supersonic.

Test Results

This generic blown HSCT model was tested subsonically over a large angle-of-attack range (−5 to +35 deg) with each canard, with each tail, and for several flap configurations on the wing and canard trailing edges. Figure 2 shows the canard locations relative to the wing LE. (Of course, on this half-span model, only one canard was tested at a time.) The majority of the tests conducted were run at a nominal freestream dynamic pressure of 20 psf, corresponding to a Reynolds number of 1.34×10^6, based on MAC = 1.716 ft.

Canard and Blowing Effects

Canards 1 and 3 (AR = 1.29 and 2.58, respectively) were evaluated at two vertical locations: high (fuselage centerline) and low (wing plane), but only with the 20-deg plain flap on the wing, and not with the CC flap installed. Figures 5 and 6 present the tail-off lift curves and drag polars for the baseline unblown aircraft (cruise and 20-deg flap), and for the 20-deg blown flap, both with and without the canards. From the data taken, the lower aspect-ratio Canard 1 was found to be the more effective of the two, apparently because its forward-swept blowing slot aligned the jet sheet and downwash more effectively with the wing LE and its vortex. The lift and drag data shown in Fig. 5 for Canard 1 are presented for no wing blowing and for wing $C_\mu = 0.328$ (lesser C_μ values were evaluated and showed less total lift but greater lift augmentation per unit of blowing momentum). Canard blowing $C_{\mu c}$ of 0.0 and 0.1 are also shown. The unblown 20-deg wing flap and Canard 1 provided an increase of approximately 33% (from $C_L = 1.06$ to 1.41) in lift and 27% in stall angle (from $\alpha = 24$ to 30.5 deg) over the unblown clean cruise configuration caused primarily by the delay of wing vortex burst, as shown by flow visualization. See Table 1 for more details. The addition of blowing to the 20-deg wing flap (canard off) increased $C_{L_{max}}$ by 65% (to $C_L = 1.74$), with little change in stall angle from the cruise configuration, whereas the unblown 20-deg flap by itself yielded only an 8% lift increase and a stall angle decrease compared with the clean aircraft. However, the real payoff occurred from combining the blown canard and the blown wing. Here, maximum C_L increased by 103% (to over 2.1), and the associated stall angle by 26% over the clean configuration. These are improvements achieved without the use of canard deflection (canard incidence = 0 deg). The data are for the blown canard with no flap deflection beyond its initial cruise configuration, i.e., they're primarily a result of blowing, not canard flap deflection. Figure 6 shows similar data for Canard 3 with AR = 2.58, where, in general, the lift performance is somewhat less and drag reductions are similar to those with Canard 1. Table 1 summarizes maximum lift, drag, and stall angle changes caused by blowing and the presence of each canard. Relative to the unblown baseline cruise configuration (0-deg flaps), these data show $C_{L_{max}}$ increases of more than 100% and stall angle increases of over 45% produced by the blown-canard/20-deg-flap configuration.

An additional advantage from these blown configurations is terminal area operation at a much lower angle of attack and the ability to vary drag coefficient as needed. From Fig. 5a, the maximum lift ($C_{L_{max}} = 1.06$) of the clean configuration occurs at $\alpha = 24$ deg, whereas wing blowing of $C_\mu = 0.328$ yields that same

Table 1 Increments caused by blown wings and Canards 1 and 3 relative to unblown baseline configuration[a]

				Canard 1			Canard 3		
Wing C_μ, $\delta_F = 20$ deg	Canard	Position	Canard $C\mu_c$	ΔC_D @ $C_L = 1.0$, %	$\Delta C_{L_{max}}$, %	$\Delta\alpha_{stall}$, %	ΔC_D @ $C_L = 1.0$, %	$\Delta C_{L_{max}}$, %	$\Delta\alpha_{stall}$, %
0.0	Off	——	0.0	−17.4	9.5	−7.5	−17.4	9.5	−7.5
0.0	On	High	0.0	−9.1	32.6	26.7	−17.4	24.5	18.3
0.0	On	Low	0.0	——	——	——	−9.1	25.5	−4.2
0.0	On	High	0.1	−27.8	52.8	32.1	−28.3	40.6	28.6
0.0	On	Low	0.1	——	——	——	−22.2	40.6	22.9
0.0	On+Flap	High	0.1	4.4	50.9	45.8	−13.0	44.3	28.6
0.0	On+Flap	Low	0.1	8.7	32.1	43.8	−4.6	34.9	31.3
0.328	Off	——	0.0	−103.3	65.1	−3.8	−103.3	65.1	−3.8
0.328	On	High	0.0	−93.5	84.0	21.3	−95.9	77.4	16.2
0.328	On	Low	0.0	——	——	——	−91.3	82.1	20.8
0.328	On	High	0.1	−106.1	102.8	25.8	−104.4	93.4	20.3
0.328	On	Low	0.1	——	——	——	−101.1	91.5	21.7
0.328	On+Flap	High	0.0	−87.4	87.7	25.0	−91.3	84.9	20.3
0.328	On+Flap	Low	0.0	−87.0	84.9	17.1	−90.9	83.0	12.5
0.328	On+Flap	High	0.1	−87.4	96.2	34.2	−91.3	95.3	20.3
0.328	On+Flap	Low	0.1	−87.0	79.3	45.8	−84.8	93.4	25.0

[a]Canard off, flap = 0 deg, $C_\mu = 0$.

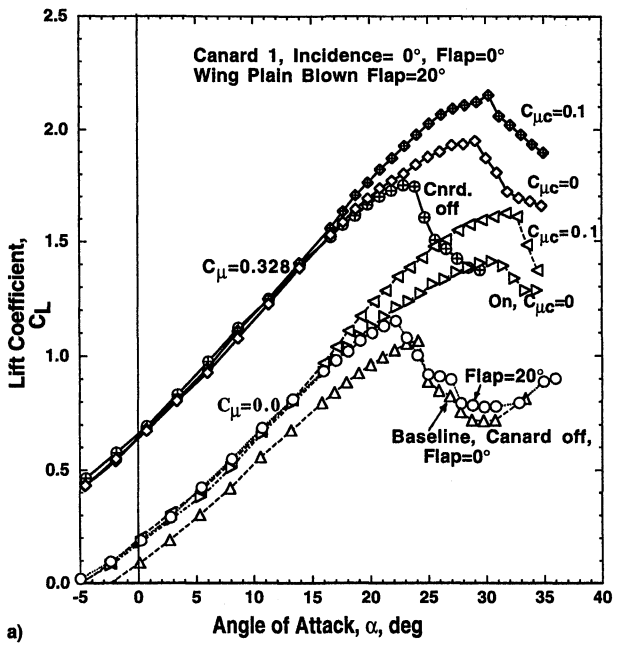

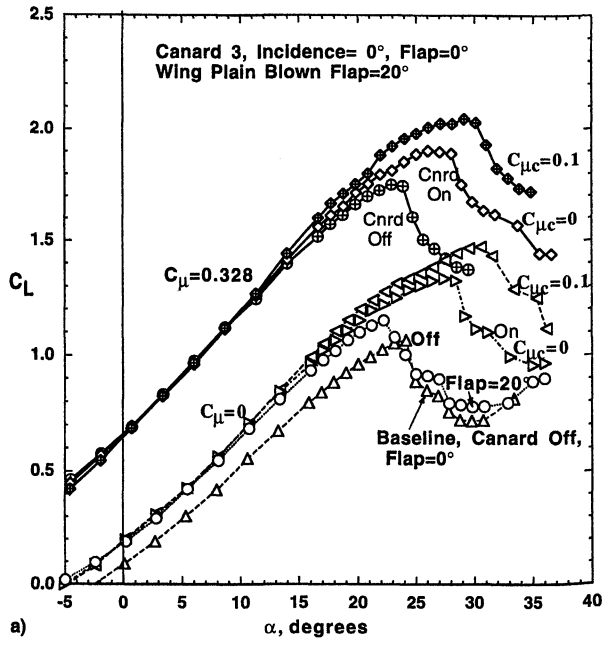

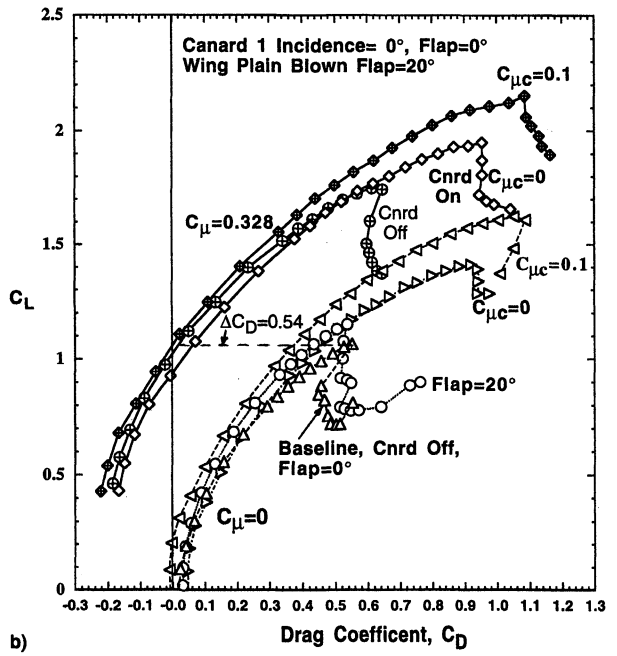

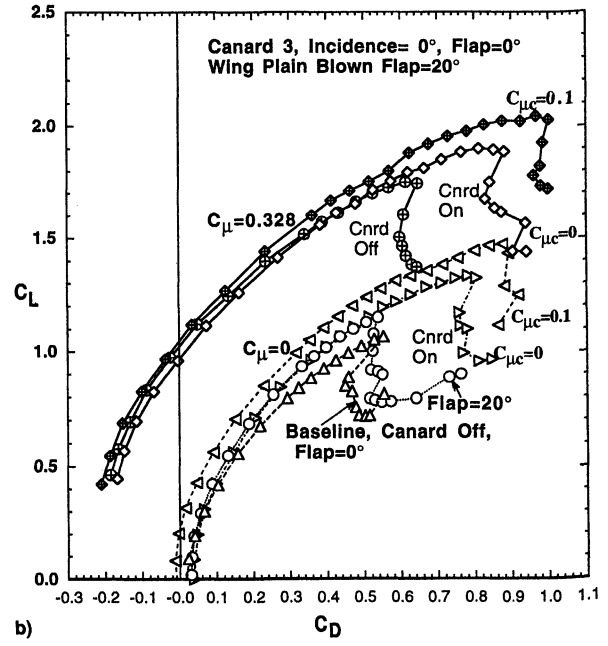

Fig. 5 Effectiveness of wing blowing, Canard 1 (AR = 1.29), and canard blowing, tail off: a) lift curves and b) drag polars.

Fig. 6 Effectiveness of wing blowing, Canard 3 (AR = 2.58), and canard blowing, tail off: a) lift curves and b) drag polars.

C_L at α = 8 deg. Significant drag reduction is also possible (Fig. 5b). At the maximum lift value of the clean configuration, wing blowing alone (C_μ = 0.328, no canard) reduces the drag from C_D = 0.56 to 0.02. This represents apparent drag reductions of 96%, or more than 160% of the blowing momentum (thrust) employed, but is a combination of blowing thrust recovery and lower angle of attack on the wing and fuselage. At that same drag value for the clean configuration (C_D = 0.56 at $C_{L_{max}}$), the lift can be increased from C_L = 1.06 to 1.80 (70%) by use of wing and canard blowing. Proper adjustment of canard and wing blowing could optimize *L/D* values for both takeoff and landing flight paths.

The main gain from the canard is confirmed by the vortex characteristics shown in Fig. 7. This wind-on flow visualization showed that when canard blowing was applied, the strong downwash behind the canard greatly delayed or prevented vortex burst on the wing because of the reduced upwash over the swept LE. Figure 7a shows a large vortex burst formation on much of the unblown wing without canard blowing at α = 29 deg, which is beyond the unblown stall angle (see Fig. 6a). In Fig. 7b, the unburst vortex is restored and the stall angle is extended by the addition of canard blowing. Figure 8 compares the lift performance of the two blown canards (with flaps deflected) and emphasizes the effect of different vertical locations. The higher position is more favorable in terms of aligning the canard downwash with the wing LE.

One additional capability of the blown canard is longitudinal pitch trim. Whereas conventional tails usually require download and lift loss to trim, a canard, particularly when blown, generates nose-up pitch and a positive lift increment to trim. Figure 9 shows that for a moment center location of 0.50 MAC, the baseline flapped configuration (tail-off) is neutrally stable, but with an untrimmed nose-down pitching moment. Addition of the canard provides nose-up pitch and trim capability, and blowing the canard enhances this trim capability. Use of canard incidence (i_c) would offer further trimming

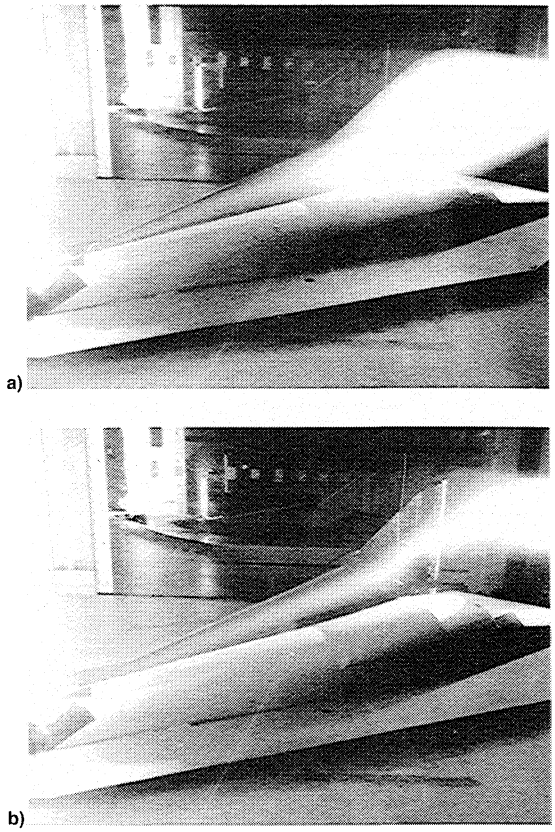

Fig. 7 Flow visualization showing vortex formation before and after canard blowing, α = 29 deg: a) no canard or wing blowing, vortex burst on wing, and b) canard blowing, unburst vortex on wing.

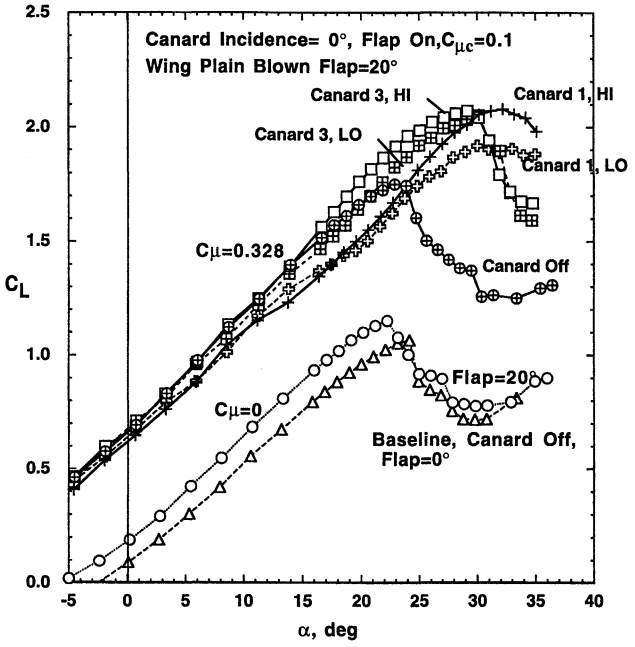

Fig. 8 Comparison of blown canards (with CC flaps) and baseline aircraft lift performance, tail off.

power. With the wing flap blown at C_μ = 0.328, only the blown canard is able to trim the aircraft at this high lift level. As will be seen, the conventional tail was inadequate for trim here.

Tail Effectiveness

In a second phase of the present test, the ability of a conventional all-flying horizontal tail (i.e., the entire slab tail pitches about a pivot axis) with no elevators to trim this aircraft was evaluated. As seen in Fig. 1, a tail with volume coefficient V_H of 0.1312 and a larger one with a 50% increase in tail area (V_H = 0.2059) were evaluated. The baseline tail in Fig. 10 restores longitudinal stability over the α range up to stall, but is inadequate to trim the unblown aircraft even when deflected (variable i_T). A 50% tail enlargement does trim the unblown aircraft (Fig. 11), but not when wing blowing is applied (data not shown). This enlarged tail also would require additional weight, structure, and a cruise drag penalty. Figure 12a compares the conventional baseline tail with the nose-up pitch capability of the canard, using either canard incidence or canard blowing. Adequate nose-up pitch trim is available from the canard, but the aircraft is longitudinally unstable at this c.g. location. Combinations of a smaller blown canard, a small horizontal tail, or farther aft c.g. are suggested. Figure 12b shows the corresponding lift values, where the canard, blown or unblown, provides significant lift and stall angle increases.

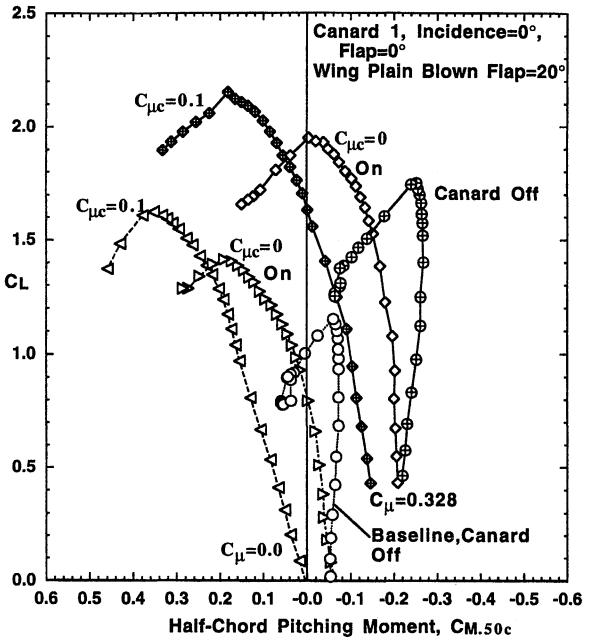

Fig. 9 Canard 1 pitch trim capability, 20-deg wing flap, tail off.

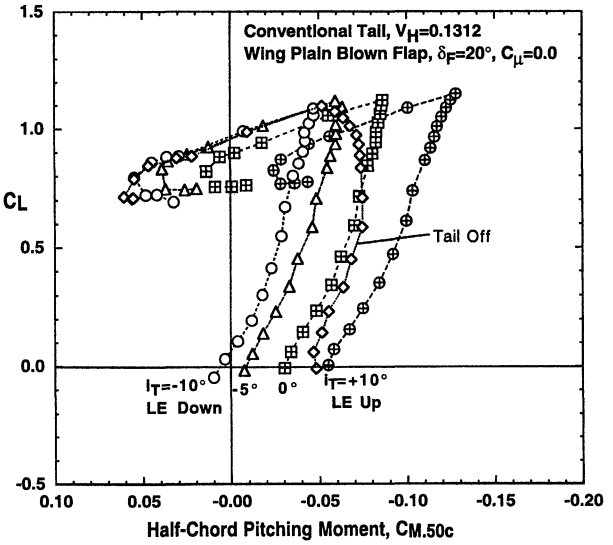

Fig. 10 Pitch provided by baseline horizontal tail, V_H = 0.1312.

Circulation Control Wing

Evaluation of an advanced blown wing was undertaken as a third phase of this test program, conducted without canards.

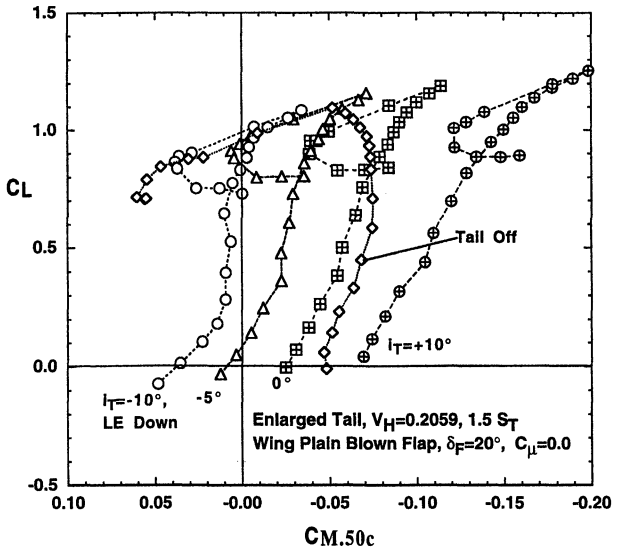

Fig. 11 Pitch and trim provided by enlarged horizontal tail, V_H = 0.2059.

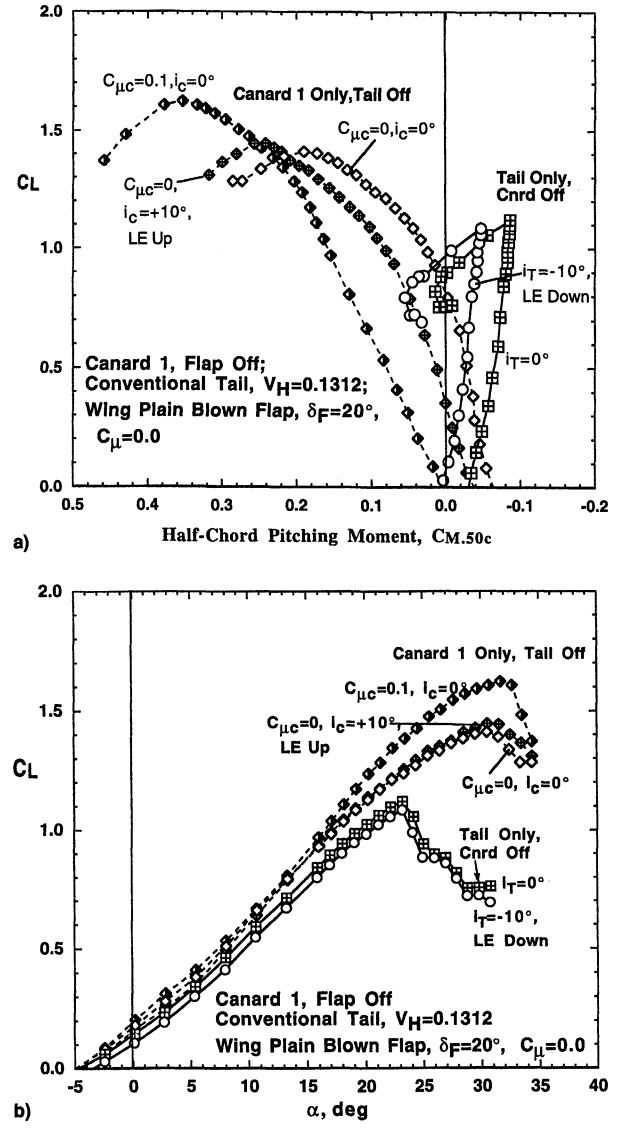

Fig. 12 Comparison of pitch trim and lift provided by baseline horizontal tail and by blown canard 1: a) half-chord pitching moment C_{M50} and b) lift curves.

Based on the very high lift augmentation already confirmed for rounded-trailing-edge circulation control wing, (CCW) configurations,[6-10] but designed to keep cruise drag low, the CCW-flapped configuration of Fig. 3 was applied to the HSCT model. In its cruise mode (δ_{Flap} = 0 deg), the trailing-edge circular arc provided 48 deg of surface arc deflection; if that arc was extended by deflection of the lower surface by about 34 deg, i.e., δ_{Flap} = 34 deg, then the jet turning angle would be 90 deg. This jet turning amount was confirmed by static flow visualization. The additional flap deflection is intended to provide much greater lift augmentation and drag generation for use on approach. Figure 13 shows how the additional jet turning of the three pneumatic flap configurations augments lift at α = 0 deg. The flapped CCW with blowing nearly doubles the lift of the undeflected CCW because of the additional

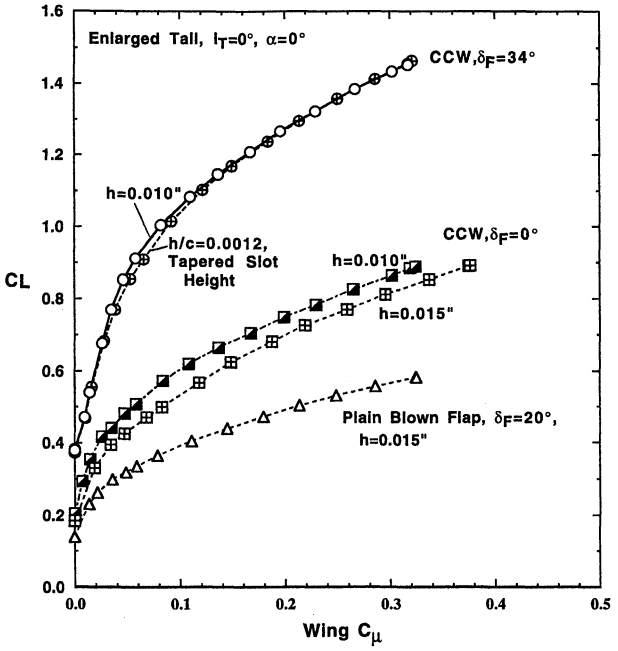

Fig. 13 Lift augmentation caused by various blown wing TE flaps, α = 0, enlarged tail, canard off.

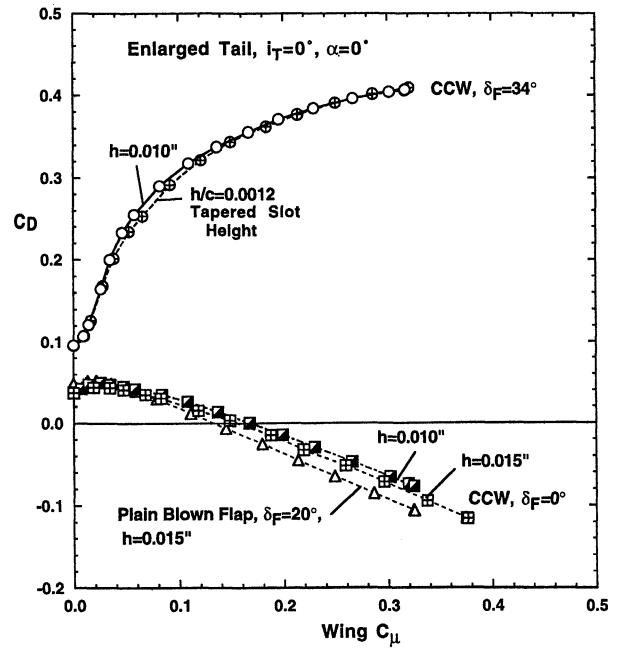

Fig. 14 Drag variation caused by various blown wing TE flaps, α = 0, enlarged tail, canard off.

jet turning, nearly triples the lift of the 20-deg plain blown flap, and multiples the lift of the unblown 20-deg plain flap by a factor of more than 10. The effect of slot height variation is also seen here, including slot height linear reduction with span and local wing chord (h/c = 0.0012). Notice that for the moderate blowing values for the 34-deg CCW flap, lift augmentation of 12 times the jet blowing momentum was achieved, i.e., $\Delta C_L/C_\mu$ = 1200%. Nose-down pitching moment (data not shown) was seen to increase with lift because of the increased aft loading produced by blowing. The ability of these three blown configurations to alter drag is shown in Fig. 14, where the additional jet turning and lift also add to the induced drag. The cruise CCW configuration and the 20-deg plain blown flap (lower curves) both reduce drag because of less jet deflection and more thrust recovery.

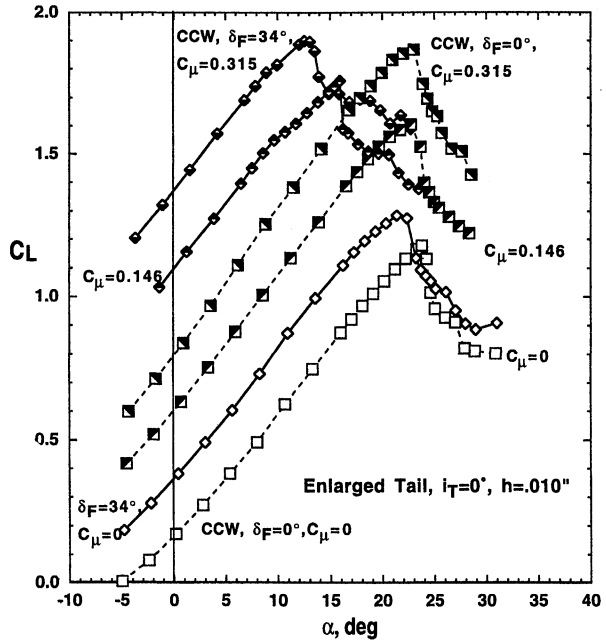

Fig. 15 Lift variation for two CCW flap deflections, canard off.

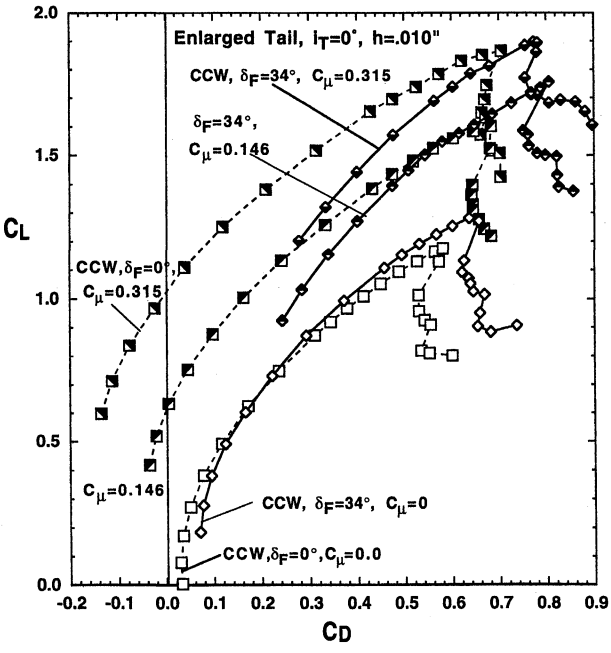

Fig. 16 Drag polars for two CCW flap deflections, canard off.

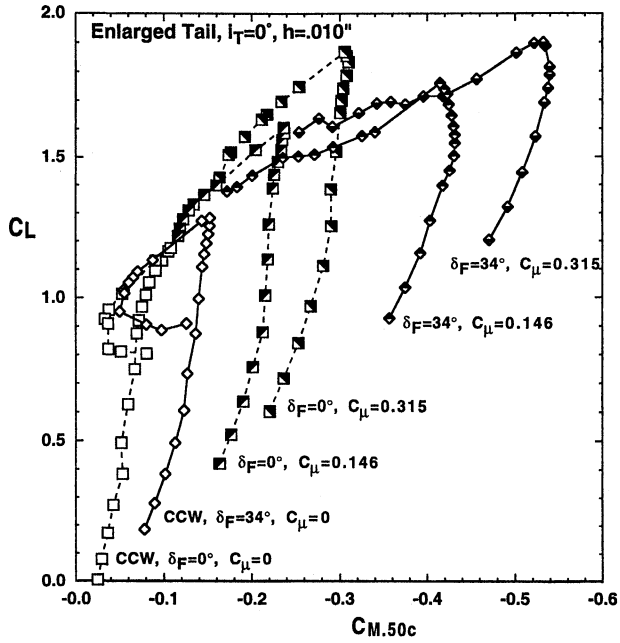

Fig. 17 Pitching moment variation for two CCW flap deflections, canard off.

Figures 15–17 present variations in lift, drag, and pitching moment at constant wing C_μ values over a range of incidence for the two CCW configurations (δ_F = 0 and 34 deg). Drag and pitch characteristics are similar to the comparisons made in previous figures when flap deflection was varied. However, lift and stall angle show a new trend: for δ_F = 0 deg, the stall angle is relatively constant as C_μ increases, but for the greater flap deflection (34 deg), the stall angle reduces as C_μ increases. Lift augmentation caused by either α or C_μ appears to reach a limit near C_L = 1.9 for this wing. It is surmised that this limit is related to increased vortex strength as a result of circulation. Thus, even if the greater flap deflection yields much higher lift at lower incidence, overall maximum wing circulation and lift appear to be limited. This limitation appears to be independent of how that wing C_L is reached (by incidence, blowing, or flap deflection). However, returning to Figs. 5, 6, and 8, higher lift up to C_L = 2.2 can be achieved if the canard is used to carry part of the lift and to reduce the upwash angles at the swept LEs, thus preventing the vortex breakdown. It would appear that control of vortex breakdown is an essential factor in generating higher lift on these highly swept wings. Devices such as wing LE vortex flaps[13] or blown LEs[4] might prove useful here.

Summary and Conclusions

Subsonic evaluations of blown lift and control surfaces applied to highly swept generic HSCT configurations have confirmed that blowing can significantly augment both force generation and control capability for these configurations. From these results, it is evident that a blown canard in combination with a blown vortex-generating wing can dramatically increase both lift and stall angle of HSCT-type aircraft by use of pneumatic force augmentation and by delay of swept-wing vortex burst. Dramatic drag reductions even greater than full thrust recovery are possible as well.

Relative to the cruise baseline HSCT configuration, these blown devices have shown significant improvements, including the following:

1) $C_{L_{max}}$ increases of more than 100% and stall angle increases of greater than 45%, resulting from a combination of blown canard and blown flap ability to augment circulation while delaying stall caused by vortex burst. Lift augmentation values ($\Delta C_L/C_\mu$) measured on these highly swept wings show

a 1200% return on the blowing momentum input for the CCW configurations.

2) Drag reductions greater than 100% at constant C_L, partly caused by jet thrust recovery and partly caused by operation at much lower body and wing incidence to achieve a desired lift coefficient.

3) Lift generation at a much lower angle of attack, reducing the need for such typical HSCT characteristics as high-α approaches, drooped noses, and aft fuselage upsweep.

4) Blown canards (or even unblown canards) appear able to trim the nose-down pitch of these configurations, as well as to limit the circulation-induced upwash and, thus, delay stall caused by vortex bursting.

Additional trends observed were as follows:

1) Neither the conventional nor the enlarged horizontal tails were able to trim this generic HSCT configuration in the high-lift modes tested. Unless canards were added, only the unblown 20-deg plain flap configuration was trimmable using only the tails. The canards alone provided the necessary trim capability, but were longitudinally unstable. A mutually beneficial combination of the two control surfaces, possibly of reduced size, is suggested.

2) Aerodynamic lift for the wing/tail combination without canards appeared to reach a vortex-burst-induced limiting value for this configuration, independent of how the wing circulation was achieved (incidence, blowing, flaps, etc.). Canards helped the configuration to exceed this limit by reducing upwash onto the wing, delaying vortex burst, and carrying additional lift load.

It has thus been shown that pneumatic high-lift devices and control surfaces offer significant improvements in the low-speed characteristics of HSCT-type aircraft. However, vortex burst and stall need to be controlled, and some form of leading-edge device or canard could be considered. Conventional tail surfaces alone do not appear adequate to trim the high-lift devices evaluated and, thus, a blown canard integrated with or replacing this tail looks quite promising.

References

[1]Campbell, J. F. "Augmentation of Vortex Lift by Spanwise Blowing," *Journal of Aircraft*, Vol. 13, No. 9, 1976, pp. 727–732.

[2]Rao, D. M., "Pneumatic Concept for Tip-Stall Control of Cranked-Arrow Wings," *Journal of Aircraft*, Vol. 31, No. 6, 1994, pp. 1380–1386.

[3]Cornelius, K. C., Pandit, N., Osborn, R. F., and Guyton, R. W., "Experimental Study of Pneumatic Control of Forebody Vortices at High Alpha," *Journal of Aircraft*, Vol. 31, No. 1, 1994, pp. 49–56.

[4]Tavella, D. A., "Lift of Delta Wings with Leading-Edge Blowing," *Journal of Aircraft*, Vol. 25, No. 6, 1988, pp. 522–524.

[5]Banks, D. W., and Paulson, J. P., Jr., "Approach and Landing Technologies for STOL Fighter Configurations," *Journal of Aircraft*, Vol. 22, No. 4, 1985, pp. 277–282.

[6]Englar, R. J., Smith, M. J., Kelley, S. M., and Rover, R. C., III, "Application of Circulation Control Technology to Advanced Subsonic Transport Aircraft, Part I: Airfoil Development," *Journal of Aircraft*, Vol. 31, No. 5, 1994, pp. 1160–1168.

[7]Englar, R. J., and Huson, C. G., "Development of Advanced Circulation Control Wing High-Lift Airfoils," *Journal of Aircraft*, Vol. 21, No. 7, 1984, pp. 476–483.

[8]Englar, R. J., Hemmerly, R. A., Moore, W. H., Seredinsky, V., Valckenaere, W. G., and Jackson, J. A., "Design of the Circulation Control Wing STOL Demonstrator Aircraft," AIAA Paper 79-1842, Aug. 1979.

[9]Englar, R. J., and Applegate, C. A., "Circulation Control—A Bibliography of David Taylor Naval Ship R&D Center (DTNSRDC) Research and Selected Outside References (January 1969 to December 1983)," DTNSRDC-84/052, Sept. 1984.

[10]Englar, R. J., "Application of Pneumatic Lift and Control Surface Technology to Advanced Transport Aircraft," *Transportation Beyond 2000: Technologies Needed for Engineering Design*, NASA CP-10184, Feb. 1996.

[11]Englar, R. J., Smith, M. J., Kelley, S. M., and Rover, R. C., III, "Application of Circulation Control Technology to Advanced Subsonic Transport Aircraft, Part II: Transport Application," *Journal of Aircraft*, Vol. 31, No. 5, 1994, pp. 1169–1177.

[12]Pugliese, A. J., and Englar, R. J., "Flight Testing the Circulation Control Wing," AIAA Paper 79-1871, Aug. 1979.

[13]Campbell, J. F., Osborn, R. F., and Foughner, J. T., Jr. (eds.), *Vortex Flow Aerodynamics, Volume I*, NASA CP 2416, Oct. 1985.